Acta Biochim Biophys Sin 2023, 55(3): 417–425
https://doi.org/10.3724/abbs.2022157
Advance Access Publication Date: 26 October 2022
Original Article

Original Article

Secreted phosphoprotein 1 promotes angiogenesis of glioblastoma through upregulating PSMA expression via transcription factor HIF1α

Wenjing Tu[1,2,†], Hui Zheng[3,†], Liangdong Li[1,2], Changshuai Zhou[1,2], Mingtao Feng[1,2], Lei Chen[1,2], Deheng Li[1,2], Xin Chen[1,2], Bin Hao[1,2], Huaping Sun[4,*], Yiqun Cao[1,2,*], and Yang Gao[1,2,*]

[1]Department of Neurosurgery, Fudan University Shanghai Cancer Center, Shanghai 200032, China, [2]Department of Oncology, Shanghai Medical College, Fudan University, Shanghai 200032, China, [3]Department of Nuclear Medicine, Shanghai Tenth People's Hospital, Tongji University, Shanghai 200072, China, and [4]Department of Radiology, Huashan Hospital, Fudan University, Shanghai 200040, China

[†]These authors contributed equally to this work.

*Correspondence address. Tel: +86-15821960178; E-mail: baiyizhanshi@126.com (Y.G.) / Tel: +86-18121299343; E-mail: gem23@163.com (Y.C.) / Tel: +86-18121186619; E-mail: 452812668@qq.com (H.S.)

Received 4 July 2022 Accepted 15 August 2022

Abstract

Glioblastoma multiforme (GBM) is a highly vascularized malignant brain tumor. Our previous study showed that prostate-specific membrane antigen (PSMA) promotes angiogenesis of GBM. However, the specific mechanism underlying GBM-induced PSMA upregulation remains unclear. In this study, we demonstrate that the GBM-secreted cytokine phosphoprotein 1 (SPP1) can regulate the expression of PSMA in human umbilical vein endothelial cells (HUVECs). Our mechanistic study further reveals that SPP1 regulates the expression of PSMA through the transcription factor HIF1α. Moreover, SPP1 promotes HUVEC migration and tube formation. In addition, HIF1α knockdown reduces the expression of PSMA in HUVECs and blocks the ability of SPP1 to promote HUVEC migration and tube formation. We further confirm that SPP1 is abundantly expressed in GBM, is associated with poor prognosis, and has high clinical diagnostic value with considerable sensitivity and specificity. Collectively, our findings identify that the GBM-secreted cytokine SPP1 upregulates PSMA expression in endothelial cells via the transcription factor HIF1α, providing insight into the angiogenic process and promising candidates for targeted GBM therapy.

Key words glioblastoma multiforme, SPP1, PSMA, angiogenesis, HIF1α

Introduction

Glioblastoma multiforme (GBM) is a highly invasive and devastatingly aggressive malignant brain tumor with an increasing incidence and a short median overall survival of approximately 16 months after diagnosis [1]. Despite a series of optimal treatments, including radical surgical resection combined with standard radiotherapy and chemotherapy, the median survival of patients remains poor [2].

Unlike extracranial cancers, GBM infiltrates deeply into the surrounding brain parenchyma and rarely metastasizes out of the brain [3]. The extraordinary patterns of diffuse infiltration and recurrence are partly ascribed to tortuous blood vessels of GBM, which provide migration routes for tumor cells [4]. GBM is one of the highly vascularized tumors due to the tumor-derived upregulation of angiogenic receptors and factors that stimulate angiogenesis signaling, such as vascular endothelial growth fact (VEGF), fibroblast growth factor (FGF), and angiopoietin-1 [5–9]. Hence, antiangiogenesis therapies have attracted broad interest because of the correlation of angiogenesis with GBM prognosis and ease of exposure to targeted drugs [10–12]. However, since GBM is a highly heterogeneous and complex tumor with particularly invasive properties, most antiangiogenic therapies have hitherto limited

efficacy in clinical trials [13,14]. Furthermore, most antiangiogenic therapies target vascular endothelial growth factor (VEGF), and other effective molecular candidates need to be explored further [9]. Hence, in-depth investigations of the molecular mechanism underlying GBM angiogenesis are conducive to identifying effective treatments.

Our previous study revealed that prostate-specific membrane antigen (PSMA) plays a pivotal role in GBM angiogenesis [15]. PSMA, encoded by the gene folate hydrolase 1 (FOLH1), is a type II transmembrane glycoprotein acting as a glutamate carboxypeptidase on different substrates, including the nutrient folate and neuropeptide N-acetyl-L-aspartyl-L-glutamate [16]. PSMA overexpression in endothelial cells has been associated with aggressiveness and rich neovasculature in various cancers [17–20]. In our previous study, we demonstrated that PSMA is robustly expressed in the vascular endothelial cells of GBM and significantly associated with poor prognosis [15]. A series of *in vitro* and *in vivo* experiments demonstrated that PSMA overexpression facilitates endothelial cell proliferation, migration and tube formation in GBM via interactions with integrin β4 (ITGB4) and activation of the nuclear factor (NF)-κB signaling pathway [15]. Therefore, PSMA may be of paramount importance in GBM angiogenesis and could be a potential candidate for targeted therapy. However, the upstream molecular mechanism by which GBM regulates PSMA expression and promotes angiogenesis remains unclear. Herein, we aimed to explore the mechanism of PSMA expression and its potential clinical transformation.

Materials and Methods

Cell culture and preparation of conditioned medium

Human umbilical vein endothelial cells (HUVECs), the human glioblastoma cell lines U87 and U251, and the human microglial cell line HMC3 were acquired from the Cell Bank of the Chinese Academy of Sciences (Shanghai, China). Cells were cultured in Dulbecco's modified Eagle's medium (DMEM; Gibco, Carlsbad, USA) supplemented with 10% fetal bovine serum (FBS; Gibco) and 1% penicillin-streptomycin reagent (Gibco) and incubated at 37°C in a humidified atmosphere with 5% CO_2. The medium was refreshed every two days. U87, U251, and HMC3 cells with the same number were cultured in serum-free medium for 24 h. Then, the cell supernatant was collected as conditioned medium for the experiment of the human cytokine antibody array.

Human cytokine antibody array

A human cytokine antibody array (RayBio C-Series Human Cytokine Antibody Array C5; Ray Biotech, Guangzhou, China) including 80 different cytokines was used to measure the levels of several cytokines in the conditioned medium of U87, U251 and HMC3 cells, according to the manufacturer's instructions. Next, we analyzed the 80 cytokines and ranked the top 40 cytokines according to the *P* values from small to large in the form of the heatmap. Among them, the most important cytokines with a significant difference were SPP1, TNFα, G-CSF, ENA-78, and NT-3, while the other cytokines had no significant difference. Analysis was performed using R and the limma package (an R package for differential analysis).

RNA isolation and quantitative real-time PCR

Total RNA was extracted using Trizol reagent (Invitrogen, Carlsbad, USA). The RNA quality and quantity were evaluated as previously described [15]. Quantitative real-time PCR was also performed as previously described [15]. The expression levels of targeted genes were assessed and *GAPDH* was used as a control. All reactions were run in triplicate. The primer sequences were as follows: *h-GAPDH*-F, 5′-ACAACTTTGGTATCGTGGAAGG-3′, and *h-GAPDH*-R, 5′-GCCATCACGCCACAGTTTC-3′; *h-PSMA*-F, 5′-ACACAGATACCA CATTTAGCAGG-3′, and *h-PSMA*-R, 5′-TTTGGGTAGGACAACAG GACA-3′; and *h-HIF1α*-F, 5′-ATCCATGTGACCATGAGGAAATG-3′, and *h-HIF1α*-R, 5′-TCGGCTAGTTAGGGTACACTTC-3′.

Protein extraction and western blot analysis

Cell pellets were washed twice with cold PBS (Gibco) and then lysed in radioimmunoprecipitation assay (RIPA) buffer (Beyotime Biotechnology, Shanghai, China) supplemented with 1% phenylmethanesulfonyl fluoride (PMSF; Beyotime Biotechnology) and 1% phosphatase inhibitor on ice. The protein concentration was determined using a BCA protein assay kit (Beyotime Biotechnology). Protein samples (10 μg) were separated by SDS-PAGE and transferred to PVDF membranes as previously described [15], and then incubated with anti-PSMA (1:1000 dilution; ab133579; Abcam, Cambridge, UK), anti-HIF1α (1:1000 dilution; ab51608; Abcam), and anti-GAPDH (1:2000 dilution; ab179467; Abcam) antibodies at 4°C overnight. Membranes were washed three times with TBST and incubated with the corresponding HRP-conjugated secondary antibodies (1:5000 dilution; 7076/7074; CST, Beverly, USA) at room temperature for 2 h. The membranes were washed again and then incubated with enhanced chemiluminescence reagent (Thermo Fisher Scientific, Waltham, USA) for 1 min. Finally, the protein band images were captured and analyzed.

Cell transfection

Three siRNA oligonucleotides targeting the *HIF1α* gene and a scramble siRNA (NC) were designed by Huajin Biotechnology (Shanghai, China) and the sequences are as follows: HIF-1α-siRNA1: 5′-AAGTTCTGAACGTCGAAAAGAAA-3′; HIF-1α-siRNA2: 5′-GACATGATTTACATTTCTGATAA-3′; HIF-1α-siRNA3: 5′-CAGT GTGTTTGATTTTACTCATC-3′; and NC: 5′-TTCTCCGAACGTGT CACGT-3′. HUVECs were transfected using Lipofectamine 2000 (Invitrogen) according to the manufacturer's protocols. In brief, HUVECs were cutured in 6-well plates to 60% confluence. Mixtures containing miRNA, siRNA or NC and Lipofectamine 2000 at the recommended concentrations were added to the cells. Cells were harvested at 48 h post transfection. The transfection efficiency was assessed by RT-PCR.

Dual-luciferase reporter assay

The Dual-Luciferase Reporter Assay kit (Promega, Madison, USA) was used to evaluate promoter activity according to the manufacturer's instructions. The luciferase reporter construct PSMA-pGL3-promoter-Luc was transiently cotransfected into HUVECs grown in 96-well plates using Lipofectamine 3000 (Invitrogen). HUVECs were previously treated and grouped correspondingly (+/– HIF1α knockdown, +/– SPP1 or PBS). Both *Firefly* and *Renilla* luciferase activities were analyzed at 72 h after infection using a dual-luciferase system on GloMax Discover (Promega).

Chromatin immunoprecipitation (ChIP) assay

For ChIP analysis, HUVECs were treated with 1 μg/mL SPP1 or PBS

and harvested separately. Cell samples in each dish with 8 mL medium were fixed using 210 μL of 37% formaldehyde for 10 min, and then the fixation was stopped by addition of 400 μL of 2.5 M glycine. The mixture was slowly shaken for 2 min until the liquid turned yellow and then washed three times with precooled PBS. Next, 1 mL PBS was added to each dish, and the cells were scraped off, tranferred to EP tubes and centrifuged at 3000 *g* for 30 s. Then cells were collected and lysed with 400 μL of 1% SDS on ice for 10 min,followed by sonication on ice and centrifugation at 4400 *g* for 10 min at 4°C. Finally, 300 μL supernatant was collected. Electrophoresis was conducted to ensure that the majority of the DNA fragments were between 300–700 bp, and the rest of the supernatant was stored at −80°C.

A total of 300 μL supernatant was diluted with 0.6 mL dilution buffer containing 1 mM PMSF (Beyotime Biotechnology). Agarose A or G beads were washed three times with TE. Each EP tube was added with 300 μL chromatin, 1.2 mL dilution buffer and 80 μL beads (50% turbidness), and then mixed for 1 h at 4°C with rotation. After centrifugation at 1300 *g* for 2 min, 50 μL supernatant was obtained as input. The supernatants were divided into two portions (475 μL each), one of which was incubated with rotation overnight in a cold chamber with the anti-PSMA antibody (2 μg)and the other with the same amount of normal IgG. The precipitated DNA was recovered using a PCR purification kit (TransGen Biotech, Beijing, China) and analyzed by qRT-PCR using a SYBR Green Real-Time PCR Master Mix (Fermentas, Waltham, USA). ChIP values were normalized to their respective input values, and the fold changes in concentration were assessed based on the relative enrichment in anti-PSMA immunoprecipitates compared with control IgG immunoprecipitates.

Tube formation assay

HUVECs with or without *HIF1α* knockdown were cultured for 24 h in the presence or absence of 1 μg/mL recombinant SPP1 protein (ACROBiosystems, Shanghai, China) in a 24-well plate precoated with Matrigel (50 μL/well; Corning, Corning, USA). Capillary-like tube formation was photographed under an inverted microscope. Tube length and branching points were calculated using ImageJ software (NIH, Bethesida, USA).

Wound healing assay

HUVECs were seeded and cultured under different treatment conditions (+/− HIF1α knockdown, +/− SPP1 or PBS) in a 6-well plate and grown to 100% confluency. Then scratch wounds were created on the the cell monolayer using 200-μL pipette tips. The plate was gently washed with PBS to remove cell debris. Images were captured at 0 h and 48 h under an inverted microscope and the gap area of the wounds were analyzed to measure the cell migration.

Clinical specimens

Serum specimens were collected from normal human volunteers ($n=20$), preoperative GBM patients ($n=20$) and postoperative GBM patients within 72 h ($n=20$) and stored at −80°C. Patients ($n=20$) received surgical treatment at Fudan University Shanghai Cancer Center between January 2021 and June 2021. Informed consents were obtained from all patients and volunteers. Ethical approval was obtained from the Ethics Committee of the Fudan University Shanghai Cancer Center.

Enzyme-linked immunosorbent assay (ELISA)

ELISA was performed to assess the SPP1 levels in serum samples using a commercial kit (ELH-OPN-1; R&D Company, Minneapolis, USA) according to the manufacturer's instructions. Serum samples were diluted 25-fold and 50 μL of diluted sample was directly added to each well of the 96-well plate previously coated with anti-human SPP1 antibody provided in the kit. Finally, the absorbance values were measured at 450 nm using a microtest plate spectrophotometer (Molecular Devices VersaMax, Silicon Valley, USA). The SPP1 levels were calculated based on a standard curve.

Bioinformatics analysis

The clinical analyses of SPP1, including expression levels, Kaplan-Meier-curves of overall survival and receiver operator characteristics (ROC) curves, were performed using The Cancer Genome Atlas (TCGA) database datasets. Moreover, the high and low SPP1 expression groups were descrinated based on the mean of SPP1 expression. The correlations of targeted genes were assessed using GEPIA (http://gepia.cancer-pku.cn/). The open-access transcription factor database JASPAR (http://jaspar.genereg.net) was used to find potential transcription factors binding to the *PSMA* promotor.

Statistical analysis

Data are presented as the mean ± SD. The data were analyzed using GraphPad Prism 9.0 software, and independent Student's *t* test (two-tailed) and one-way ANOVA test were used to analyze the differences between groups. Correlation analysis was performed by Pearson and Spearman correlation analysis. $P<0.05$ was considered statistically significant.

Results

Sreening of the contributing cytokines secreted from glioma cells

We previously demonstrated that HUVECs cultured with conditioned medium from U87 and U251 glioma cells exhibited significantly higher PSMA expression than cells cultured with normal medium [15]. To identify the factors in the conditioned medium from U87 and U251 cells that affect PSMA expression in HUVECs, we used a Human Cytokine Antibody Array to screen cytokines in the conditioned medium from U87 and U251 cells and compared to those in the medium from HMC3 cells (Figure 1A). A total of 39 upregulated and 5 downregulated cytokines were identified in the conditioned medium from U87 and U251 cells (Figure 1B). A heatmap was constructed to exhibit the most significant differential cytokine levels between those in the conditioned medium from U87 and U251 cells and those in the medium from HMC3 cells (Figure 1C). The volcano plot demonstrated 4 upregulated cytokines (SPP1, G-CSF, NT-3, and TNFα) and 1 downregulated cytokine (ENA-78/CXCL5) with the most marked difference (Figure 1D).

SPP1 from glioma cells regulates PSMA expression

To identify the target more precisely, we analyzed the correlation of PSMA with cytokines (SPP1, G-CSF, TNFα, NT-3, and ENA-78) in GBM using GEPIA. Bioinformatic analyses showed that SPP1 ($R=0.28$) and TNFα ($R=0.22$) are significantly correlated with PSMA (Figure 2A). The correlations of other cytokines with PSMA are not as marked as the correlation between PSMA and SPP1 or

TNFα, whether they are upregulated or downregulated in the conditioned medium (Figure 2A,B). However, the expression level of TNFα in conditioned medium is rather low. In addition, TNFa has been found to participate in the angiogenesis process of glioma, while it is mainly secreted from glioma-associated macrophages rather than GBM cells per se [21]. Previous reports also showed that SPP1 is associated with angiogenesis in other cancers, such as colon cancer and melanoma [22,23]. Hence, we speculated that SPP1

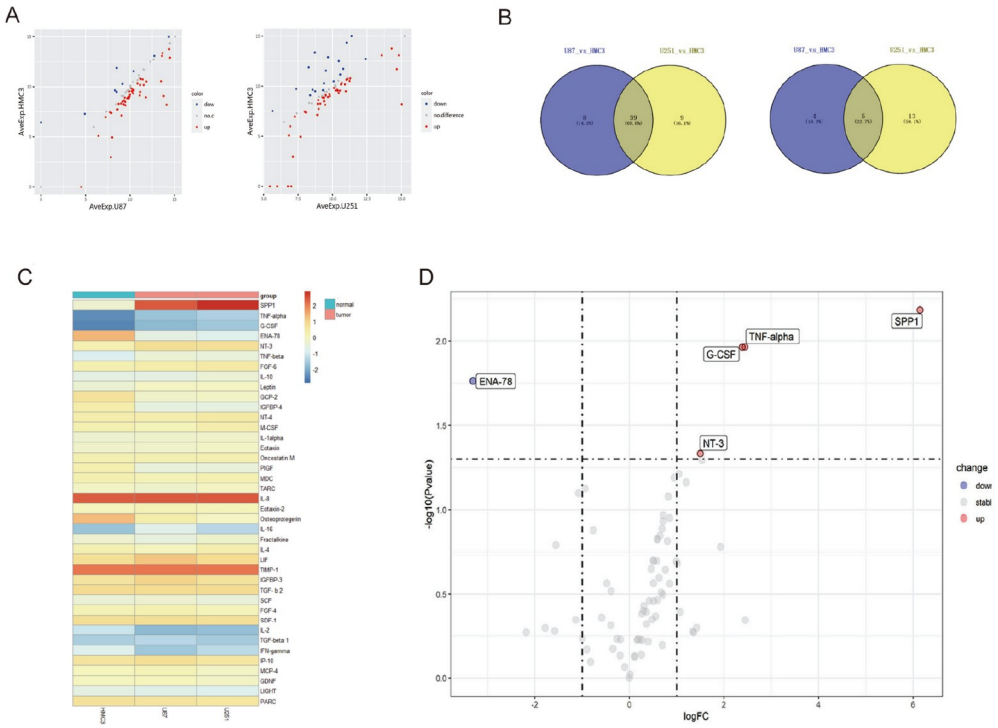

Figure 1. Screening of the contributing cytokines secreted from glioma cells (A) Human cytokine antibody array of conditioned medium from U87, U251 and HMC3 cells. (B) Analysis of 39 upregulated cytokines and 5 downregulated cytokines in conditioned medium from U87 and U251 cells. (C) Heatmap analysis of the significantly differentially expressed cytokines. (D) Volcano plot analysis of 4 markedly upregulated cytokines (SPP1, G-CSF, NT-3, and TNFα) and 1 downregulated cytokine (ENA-78).

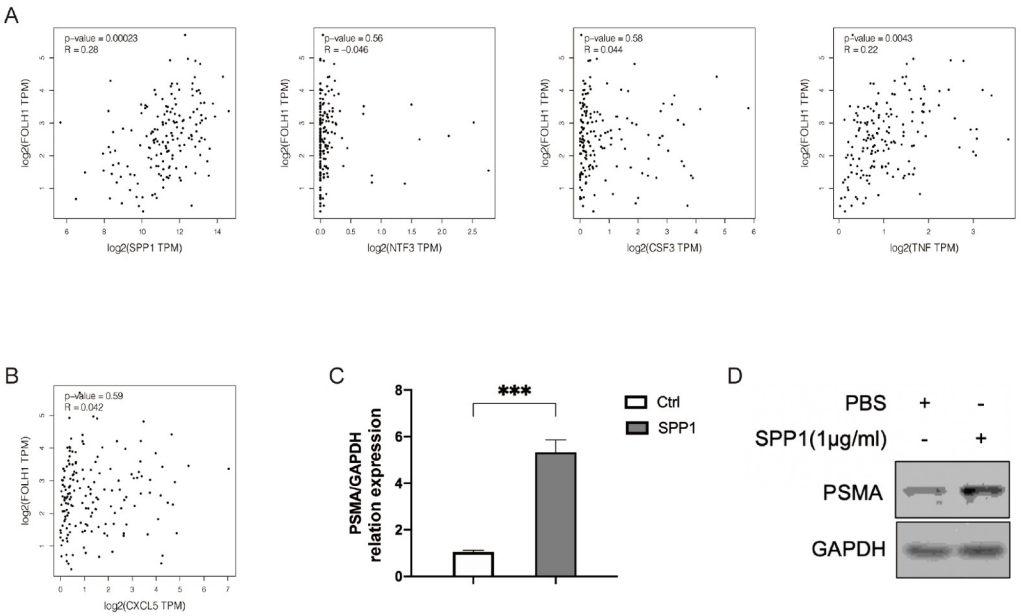

Figure 2. SPP1 from glioma cells regulates PSMA expression (A) Correlation analysis between PSMA and upregulated cytokines (SPP1, NT-3/NTF3, G-CSF/CSF3 and TNFα/TNF) in GBM by GEPIA. (B) Correlation analysis between PSMA and the downregulated cytokine ENA-78/CXCL5 in GBM by GEPIA. (C,D) The expression of PSMA after treatment with recombinant protein SPP1. ***$P < 0.001$.

might be the contributing factor. We added recombinant protein SPP1 (1 μg/mL) to the culture medium of HUVECs and PBS as a control. Accordingly, the mRNA and protein expression levels of PSMA were assessed by qRT-PCR and western blot analysis. It was found that SPP1 protein had a significant effect on PSMA upregulation in HUVECs (Figure 2C,D). Hence, glioma-secreted cytokine SPP1 was confirmed to be the contributing factor that positively upregulates PSMA in HUVECs.

SPP1 promotes PSMA upregulation through the transcription factor HIF1α

To reveal the mechanism by which SPP1 regulates PSMA expression, we sifted through the PROMO website to identify potential transcription factors that predominantly bind to the *PSMA* promoter region, and found that HIF1α could be a potent transcription factor with highly conserved binding sites in the upstream of the *PSMA* promoter region using JASPAR (Figure 3A,B). Hence, we speculated that SPP1 might upregulate the expression of PSMA through regulating HIF1α.

To verify our speculation, we knocked down *HIF1α* in HUVECs using siRNA and examined the knockdown efficiency by qRT-PCR (Figure 3C). Furthermore, we manipulated the concentration of SPP1 by adding recombinant SPP1 protein to the medium. Western blot analysis and qRT-PCR results showed that *HIF1α* knockdown mitigated the expression of PSMA (Figure 3D,E), further confirming that SPP1 upregulated the expression of PSMA, which could be reversed by knockdown of *HIF1α* (Figure 3D,E). Intriguingly, western blot analysis results showed that SPP1 alone could upregulate the expression of HIF1α, irrespective of whether *HIF1α* was knocked down or not (Figure 3D). Thus, our results confirmed that SPP1 could upregulate the expression of PSMA through enhancing HIF1α expression.

To further verify that HIF1α could bind with the *PSMA* promoter, we designed primers covering the three binding sites of the *PSMA* promoter and performed ChIP assay. The results showed that HIF1α bound to region 1 of the *PSMA* promoter (h-*PSMA*-promoter-F1, CAAATGCACGGCCTCTCTCA, and h-*PSMA*-promoter-R1, TATCCCGGCTATGTCTGGCT), which was significantly enhanced in the presence of SPP1 (Figure 3F). Dual-luciferase report gene assay was used to further assess the impact of HIF1α and SPP1 on the transcription activity of the *PSMA* promoter in HUVECs. It was found that knockdown of *HIF1α* alone decreased the relative luciferase activity which is correlated with the transcription activity of the *PSMA*-pGL3-promoter, while recombinant protein SPP1 alone had the opposite effect (Figure 3G) and the combination of downregulated HIF1α and recombinant protein SPP1 had a neutralizing effect (Figure 3G). Altogether, these results demonstrated that both SPP1 and HIF1α had a positive influence on the transcription activity of the *PSMA* promoter, also indicating that HIF1α could bind with the *PSMA* promoter.

Our findings strongly support that SPP1 upregulates the expression of PSMA through increasing the expression of HIF1α which can

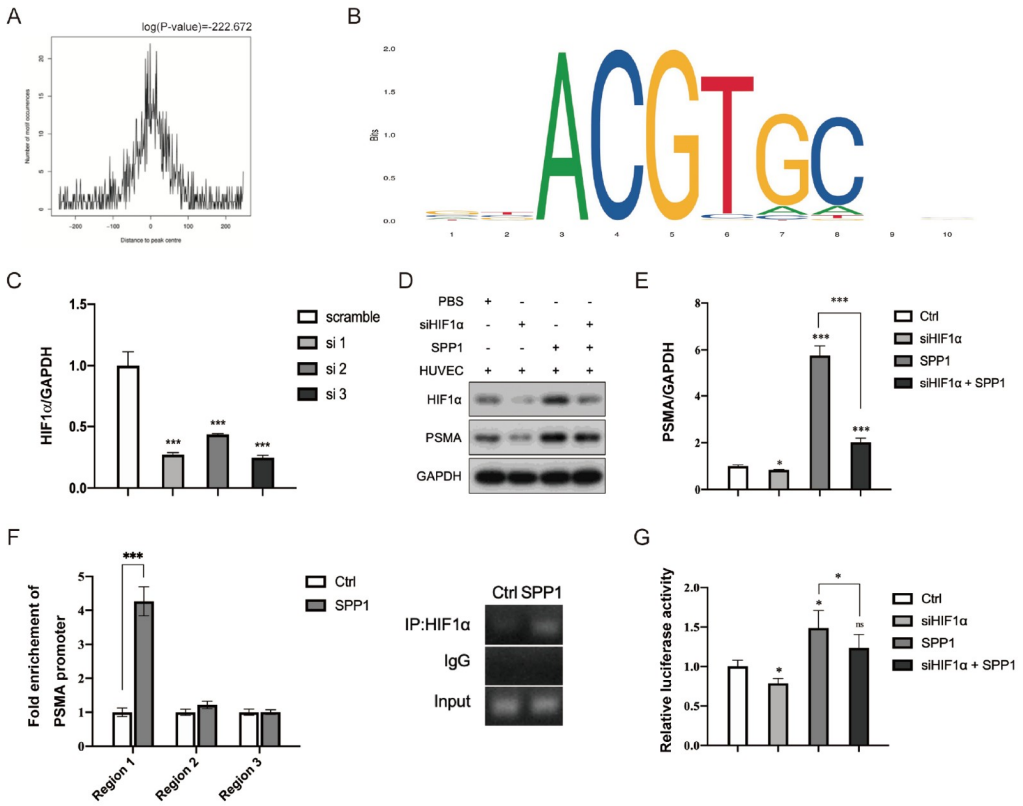

Figure 3. SPP1 promotes PSMA upregulation through the transcription factor HIF1α (A,B) Binding motif and DNA sequence of HIF1α in the promoter region of *PSMA* according to the JASPAR database. (C) The knockdown efficiency of siHIF1α in HUVECs assessed by qRT-PCR. (D) Western blot analysis was used to detect the expressions of PSMA and HIF1α proteins in HUVECs. (E) qPCR was used to detect the mRNA expression level of PSMA in HUVECs. (F) ChIP assay of the *PSMA* promoter was used to detect the binding affinity with the HIF1α antibody in the presence of SPP1. (G) The Dual-Luciferase reporter assay was used to detect transcription activity of PSMA in HUVECs. $*P<0.05$, $***P<0.001$.

bind with the *PSMA* promoter region.

SPP1-regulated endothelial cell migration and tube formation could be blocked by *HIF1α* knockdown

We previously demonstrated that PSMA overexpression affected biological functions, such as HUVEC migration and tube formation, *in vivo* and *in vitro* [15]. As mentioned above, we confirmed that GBM-secreted SPP1 could upregulate PSMA expression in HUVECs through the transcription factor HIF1α. Therefore, we hypothesized that SPP1 could also promote the migration and tube formation ability of HUVECs, which could be inhibited by knockdown of *HIF1α*. To verify this hypothesis, we added recombinant protein SPP1 (1 μg/mL) or the same volume of PBS into the culture medium of HUVECs with or without *HIF1α* knockdown. The wound healing assay showed that SPP1 promoted HUVEC migration, while downregulating HIF1α expression significantly reversed this effect (Figure 4A,C). Meanwhile, the tube formation assay showed that SPP1 significantly enhanced HUVEC tube formation. The ability of SPP1-regulated endothelial cell migration and tube formation could be blocked by knockdown of *HIF1α* (Figure 4B,D). Collectively, these results confirmed our previous speculation that GBM-released SPP1 could promote migration and tube formation of surrounding vascular endothelial cells, resulting in GBM angiogenesis and progression.

SPP1 is abundantly expressed in GBM and predicts poor prognosis

To explore SPP1 expression and its diagnostic value in GBM, we then analyzed the expression levels and prognosis of SPP1 in GBM using TCGA datasets. The results showed that SPP1 expression is higher in tumor tissues than in the normal tissues in both the low-grade glioma (LGG) and GBM groups (Figure 5A). Furthermore, Kaplan-Meier curves of overall survival indicated that high SPP1 expression is associated with poor prognosis in both the LGG and GBM groups (Figure 5B). To verify the bioinformatics results, we conducted ELISA to assess the level of SPP1 in the serum of GBM

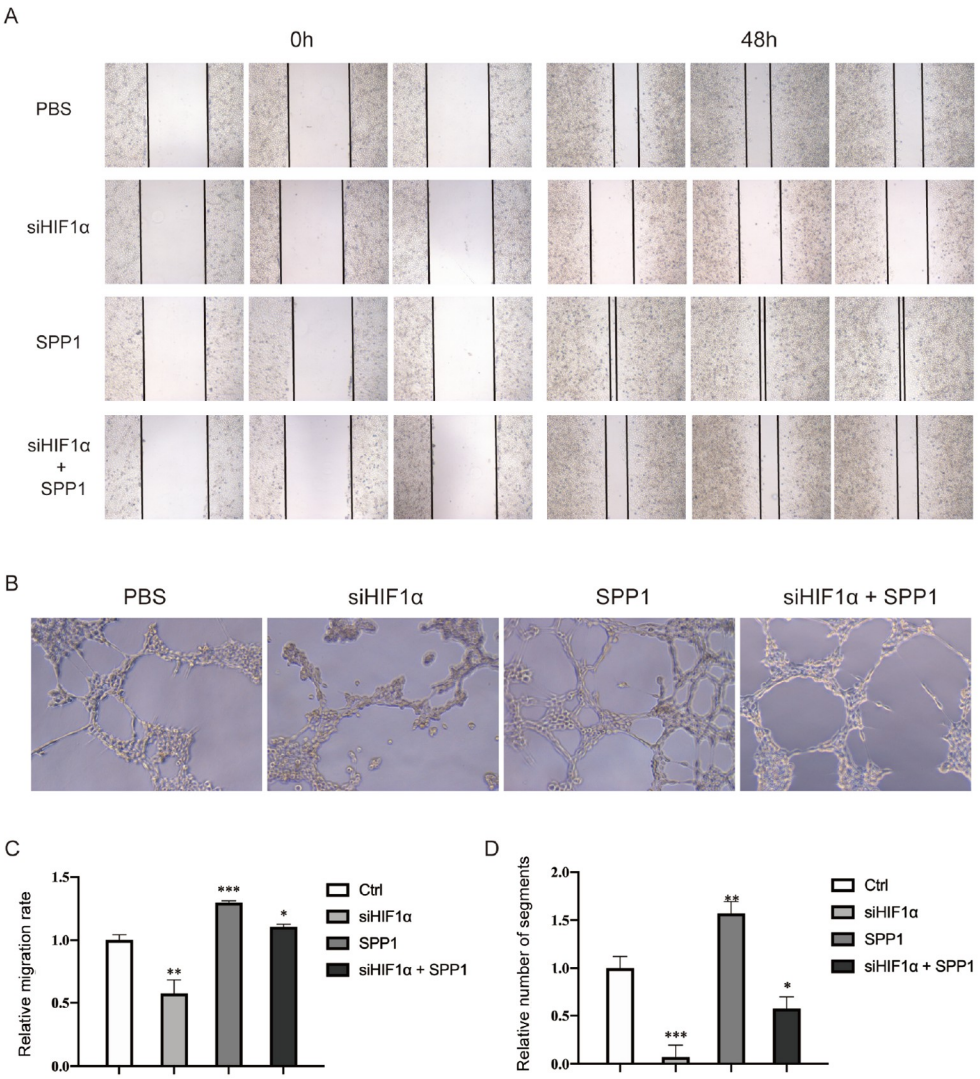

Figure 4. The ability of SPP1-regulated endothelial migration and tube formation could be blocked by *HIF1α* knockdown (A) Wound healing assay was used to detect the effect of SPP1 and HIF1α on the migration ability of HUVECs. (B) The tube formation assay was used to detect theeffect of SPP1 and HIF1α on the tube formation ability of HUVECs. (C) The statistical results of the wound healing assay. (D) The statistical results of the tube formation assay. $^{*}P<0.05$, $^{**}P<0.01$, $^{***}P<0.001$.

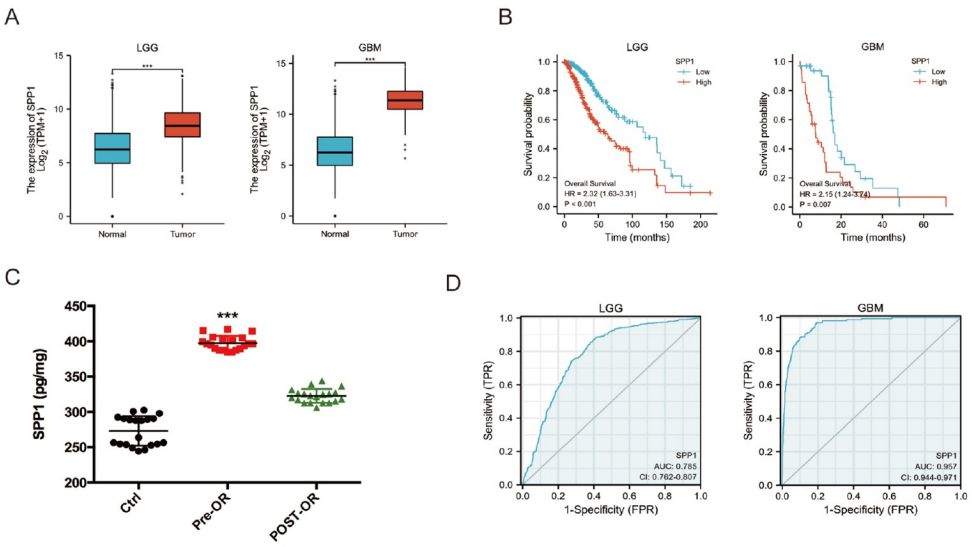

Figure 5. SPP1 is abundantly expressed in GBM and predicts poor prognosis (A) The expression of SPP1 in the LGG and GBM groups according to TCGA datasets. (B) The overall survival of SPP1 in the LGG group and GBM group by TCGA datasets. (C) The concentration of SPP1 in serum samples of normal human volunteers (Ctrl, $n = 20$), preoperative GBM patients (pre-OR, $n = 20$) and postoperative GBM patients (post-OR, $n = 20$) detected by ELISA. (D) ROC curve analysis of SPP1 in the LGG group and GBM group using TCGA datasets. ***$P < 0.001$.

patients before and after surgery, and compared with that in normal people. Compared with that in normal people, the serum level of SPP1 in preoperative GBM patients was higher. However, the serum level of SPP1 was decreased when the GBM tumor was resected (Figure 5C). The ELISA results suggested that SPP1 might be a potential diagnostic and curative biomarker in GBM patients.

To determine whether SPP1 could be used as a promising biomarker for GBM, the ROC curve was also constructed using TCGA datasets. The ROC curve demonstrated that SPP1 scores had an AUC of 0.785 [95% confidence interval (CI) = 0.762–0.807] in the LGG group and an even higher AUC of 0.957 (95% CI = 0.944–0.971) in the GBM group, indicating that SPP1 could be a potential diagnostic biomarker for GBM with high sensitivity and specificity for future clinical application (Figure 5D). Altogether, our results showed that SPP1 is abundantly expressed in GBM and predicts poor prognosis of GBM, indicating its potential as a promising target for future diagnosis of BGM with high sensitivity and specificity.

Discussion

Accumulating evidence has demonstrated that PSMA is highly expressed in the neovasculature of various cancers, including GBM [17–20,24]. Most studies focused on using PET/CT loaded with Ga-PSMA-11 or anti-PSMA minibody as an efficient imaging tool. Other studies elucidated that PSMA is highly expressed in the microvasculature of many tumors [24–27]. Our previous study demonstrated that PSMA is highly expressed in vascular endothelial cells in GBM and that it facilitates angiogenesis through interacting with ITGB4 and stimulating the NF-κB signaling pathway [15]. However, the molecular mechanism by which GBM regulates the expression of PSMA and promotes angiogenesis remains unclear.

It was reported that PSMA expression is regulated by a cis-element, the PSMA enhancer, in the prostate epithelium [28]. Moreover, PSMA enhancer can be negatively regulated by the Sox7 protein [29]. As the above mechanism is not exclusive to tumors, it is not applicable in our study to unravel the specific mechanism of GBM-induced PSMA upregulation. Our previous study demonstrated that conditioned medium from glioma cells could induce PSMA upregulation in HUVECs. Therefore, in the present study, we tried to explore the mechanism by which GBM regulates the expression of PSMA in conditioned medium from glioma cells. Supported by bioinformatics analysis and experimental verification, we confirmed that SPP1 is the pivotal GBM-derived factor that regulates PSMA expression. In addition, both the number of cells treated with SPP1 and the duration of treatment were able to affect the degree of upregulation of PSMA expression, as reveal by qRT-PCR and luciferase assays. Furthermore, SPP1 upregulated the expression of PSMA and promoted the migration and tube formation ability of HUVECs. To the best of our knowledge, this study is the first to reveal the relationship between SPP1 and PSMA.

Our study focused on the role of SPP1 in tumor angiogenesis, while in fact, SPP1 has broad biological functions in cancers, indicating its promising value in clinical diagnosis and therapy. SPP1, which has different isoforms produced by several transcript variants, is a secreted protein involved in osteoclast attachment to the mineralized bone matrix [30]. SPP1 also upregulates the expressions of interferon-γ and interleukin-12 and is involved in Th1-mediated immunity [31,32]. Many studies have revealed that SPP1 is involved in angiogenesis in tumors such as breast cancer, lung cancer, melanoma and colon cancer [22,23,33–35]. Despite the lack of mechanistic research, SPP1 has been shown to be highly associated with GBM angiogenesis [36,37], which consolidated our initial conclusion Notably, SPP1 positively upregulates VEGF expression, which is a potential mechanism of SPP1-promoted angiogenesis [36,38]. Intriguingly, PSMA-stimulated NF-κB activation is required for VEGF expression [39]. Hence, there might be a potential link between SPP1, PSMA and VEGF, which requires in-depth investigation in the future to broaden our understanding of GBM angiogenesis. Besides its role in angiogenesis, SPP1 also plays a supportive role in tumor progression processes, such as proliferation, invasion, migration and resistance to chemotherapy in multiple cancers [40–43]. Moreover, SPP1 is involved in creating

the immunosuppressed tumor microenvironment [44,45]. The abovementioned studies indicated that SPP1 might also participate in various processes of GBM progression beyond angiogenesis, inspiring us to conduct a comprehensive study of SPP1 in GBM in the future.

SPP1 is highly expressed in multiple cancers, including lung cancer, head and neck cancer, liver cancer, colon adenocarcinoma, melanoma and GBM, and correlates with poor prognosis [40,41,44–46]. We demonstrated that SPP1 is abundantly expressed in GBM compared with its level in normal tissues and positively associates with poor prognosis. Interestingly, the concentration of SPP1 in the peripheral blood of GBM patients was remarkably decreased after surgery compared with that before surgery, further demonstrating the significant clinical correlation of SPP1 with GBM. Importantly, our study is the first to assess the expression level of SPP1 in the serum of GBM patients, since previous studies focused on SPP1 expression in glioma cell lines or tissues from surgical resection [47]. Furthermore, SPP1 had a high diagnostic value in GBM with high sensitivity and specificity. In conclusion, our results indicated that serum SPP1 level combined with PSMA PET/CT is of great significance in the clinical diagnosis of GBM progression and recurrence in the future.

Through a series of rigorous studies, we proved that HIF1α is the pivotal link between SPP1 and PSMA. HIF1α is mediated by SPP1 and acts as a potent transcription factor upon binding with the *PSMA* promoter. HIF1α is known for its response to hypoxic environments to maintain homeostasis, mediating various cellular biological states, such as metabolism, inflammation and angiogenesis, and has been reported to play an essential role in tumor angiogenesis [48–50]. Because cells in hypoxic microenvironments strive for more oxygen and nutrients, newly sprouted blood vessels are needed as a pathological response to hypoxia [9]. Thus, our study provides a promising candidate for future targeted GBM diagnosis and therapy.

GBM has diffuse infiltration and a heterogeneous pattern, which makes it more likely to recur even after resection followed by radiotherapy. Compared with traditional treatment, targeting abnormal GBM angiogenesis seems to be a more promising therapy. Nevertheless, there are still a few limitations in our study. First, the number of clinical specimens is limited. Second, our experiments only confirmed the correlation between SPP1 and PSMA, while the changes in PSMA expression after treatment with different doses of SPP1 have not yet been explored, which could help verify if a dose-dependent link exists.

In summary, we identified that the upstream cytokine SPP1 secreted from GBM could upregulate PSMA expression in endothelial cells via the transcription factor HIF1α, providing insight into the angiogenic process and promising candidates for targeted GBM therapy.

Funding

This work was supported by the grants from the National Natural Science Foundation of China (Nos. 82103429 and 82173177), the Foundation of Tenth People's Hospital (No. 04.03.18.088), and the Foundation of Shanghai Municipal Health Bureau (No. 20204Y0264).

Conflict of Interest

The authors declare that they have no conflict of interest.

References

1. Vollmann-Zwerenz A, Leidgens V, Feliciello G, Klein CA, Hau P. Tumor cell invasion in glioblastoma. *Int J Mol Sci* 2020, 21: 1932
2. Khaddour K, Johanns TM, Ansstas G. The landscape of novel therapeutics and challenges in glioblastoma multiforme: contemporary state and future directions. *Pharmaceuticals* 2020, 13: 389
3. Li C, Wang S, Yan JL, Torheim T, Boonzaier NR, Sinha R, Matys T, ***et al.*** Characterizing tumor invasiveness of glioblastoma using multiparametric magnetic resonance imaging. *J Neurosurg* 2020, 132: 1465–1472
4. Cuddapah VA, Robel S, Watkins S, Sontheimer H. A neurocentric perspective on glioma invasion. *Nat Rev Neurosci* 2014, 15: 455–465
5. Takano S, Yamashita T, Ohneda O. Molecular therapeutic targets for glioma angiogenesis. *J Oncol* 2010, 2010: 1–11
6. Stacker SA, Achen MG. Emerging roles for VEGF-D in human disease. *Biomolecules* 2018, 8: 1–7
7. Lieu C, Heymach J, Overman M, Tran H, Kopetz S. Beyond VEGF: inhibition of the fibroblast growth factor pathway and antiangiogenesis. *Clin Cancer Res* 2011, 17: 6130–6139
8. Machein MR, Knedla A, Knoth R, Wagner S, Neuschl E, Plate KH. Angiopoietin-1 promotes tumor angiogenesis in a rat glioma model. *Am J Pathol* 2004, 165: 1557–1570
9. Ahir BK, Engelhard HH, Lakka SS. Tumor development and angiogenesis in adult brain tumor: glioblastoma. *Mol Neurobiol* 2020, 57: 2461–2478
10. Wang Z, Yang Z, Jiang J, Shi Z, Mao Y, Qin N, Tao TH. Silk microneedle patch capable of on-demand multidrug delivery to the brain for glioblastoma treatment. *Adv Mater* 2022, 34: 2106606
11. Sousa F, Costa-Pereira AI, Cruz A, Ferreira FJ, Gouveia M, Bessa J, Sarmento B, ***et al.*** Intratumoral VEGF nanotrapper reduces gliobastoma vascularization and tumor cell mass. *J Control Release* 2021, 339: 381–390
12. Frisch A, Kälin S, Monk R, Radke J, Heppner FL, Kälin RE. Apelin controls angiogenesis-dependent glioblastoma growth. *Int J Mol Sci* 2020, 21: 4179
13. Parker JJ, Canoll P, Niswander L, Kleinschmidt-DeMasters BK, Foshay K, Waziri A. Intratumoral heterogeneity of endogenous tumor cell invasive behavior in human glioblastoma. *Sci Rep* 2018, 8: 18002
14. Ameratunga M, Pavlakis N, Wheeler H, Grant R, Simes J, Khasraw M. Anti-angiogenic therapy for high-grade glioma. *Cochrane Database Systatic Rev* 2018, 2018: CD008218
15. Gao Y, Zheng H, Li L, Feng M, Chen X, Hao B, Lv Z, ***et al.*** Prostate-specific membrane antigen (PSMA) promotes angiogenesis of glioblastoma through interacting with ITGB4 and regulating NF-κB signaling pathway. *Front Cell Dev Biol* 2021, 9: 598377
16. Hyväkkä A, Virtanen V, Kemppainen J, Grönroos TJ, Minn H, Sundvall M. More than meets the eye: scientific rationale behind molecular imaging and therapeutic targeting of prostate-specific membrane antigen (PSMA) in metastatic prostate cancer and beyond. *Cancers* 2021, 13: 2244
17. Chang SS, Reuter VE, Heston WD, Bander NH, Grauer LS, Gaudin PB. Five different anti-prostate-specific membrane antigen (PSMA) antibodies confirm PSMA expression in tumor-associated neovasculature. *Cancer Res* 1999, 59: 3192–3198
18. Conway RE, Rojas C, Alt J, Nováková Z, Richardson SM, Rodrick TC, Fuentes JL, ***et al.*** Prostate-specific membrane antigen (PSMA)-mediated laminin proteolysis generates a pro-angiogenic peptide. *Angiogenesis* 2016, 19: 487–500

19. Wernicke AG, Varma S, Greenwood EA, Christos PJ, Chao KS, Liu H, Bander NH, *et al.* Prostate-specific membrane antigen expression in tumor-associated vasculature of breast cancers. *APMIS* 2014, 122: 482–489
20. Watanabe R, Maekawa M, Kiyoi T, Kurata M, Miura N, Kikugawa T, Higashiyama S, *et al.* PSMA-positive membranes secreted from prostate cancer cells have potency to transform vascular endothelial cells into an angiogenic state. *Prostate* 2021, 81: 1390–1401
21. Wei Q, Singh O, Ekinci C, Gill J, Li M, Mamatjan Y, Karimi S, *et al.* TNFα secreted by glioma associated macrophages promotes endothelial activation and resistance against anti-angiogenic therapy. *Acta Neuropathol Commun* 2021, 9: 67
22. Wu XL. Osteopontin knockdown suppresses the growth and angiogenesis of colon cancer cells. *World J Gastroenterol* 2014, 20: 10440
23. Kale S, Raja R, Thorat D, Soundararajan G, Patil TV, Kundu GC. Osteopontin signaling upregulates cyclooxygenase-2 expression in tumor-associated macrophages leading to enhanced angiogenesis and melanoma growth via α9β1 integrin. *Oncogene* 2014, 33: 2295–2306
24. Sasikumar A, Kashyap R, Joy A, Charan Patro K, Bhattacharya P, Reddy Pilaka VK, Oommen KE, *et al.* Utility of 68Ga-PSMA-11 PET/CT in imaging of glioma—a pilot study. *Clin Nucl Med* 2018, 43: e304–e309
25. Nomura N, Pastorino S, Jiang P, Lambert G, Crawford JR, Gymnopoulos M, Piccioni D, *et al.* Prostate specific membrane antigen (PSMA) expression in primary gliomas and breast cancer brain metastases. *Cancer Cell Int* 2014, 14: 26
26. Matsuda M, Ishikawa E, Yamamoto T, Hatano K, Joraku A, Iizumi Y, Masuda Y, *et al.* Potential use of prostate specific membrane antigen (PSMA) for detecting the tumor neovasculature of brain tumors by PET imaging with 89Zr-Df-IAB2M anti-PSMA minibody. *J Neurooncol* 2018, 138: 581–589
27. Kunikowska J, Bartosz K, Leszek K. Glioblastoma multiforme: another potential application for 68Ga-PSMA PET/CT as a guide for targeted therapy. *Eur J Nucl Med Mol Imag* 2018, 45: 886–887
28. Watt F, Martorana A, Brookes DE, Ho T, Kingsley E, O'Keefe DS, Russell PJ, *et al.* A tissue-specific enhancer of the prostate-specific membrane antigen gene, FOLH1. *Genomics* 2001, 73: 243–254
29. Peng W, Guo L, Tang R, Liu X, Jin R, Dong JT, Xing CG, *et al.* Sox7 negatively regulates prostate-specific membrane antigen (PSMA) expression through PSMA-enhancer. *Prostate* 2019, 79: 370–378
30. Denhardt DT, Noda M. Osteopontin expression and function: role in bone remodeling. *J Cell Biochem* 1998, 102: 92–102
31. Maeno Y, Nakazawa S, Dao LD, Van Tuan N, Giang ND, Van Hanh T, Taniguchi K. Osteopontin is involved in Th1-mediated immunity against Plasmodium falciparum infection in a holoendemic malaria region in Vietnam. *Acta Tropica* 2006, 98: 305–310
32. Renkl AC, Wussler J, Ahrens T, Thoma K, Kon S, Uede T, Martin SF, *et al.* Osteopontin functionally activates dendritic cells and induces their differentiation toward a Th1-polarizing phenotype. *Blood* 2005, 106: 946–955
33. Krstic M, Hassan HM, Kolendowski B, Hague MN, Anborgh PH, Postenka CO, Torchia J, *et al.* Isoform-specific promotion of breast cancer tumorigenicity by TBX3 involves induction of angiogenesis. *Lab Invest* 2020, 100: 400–413
34. Raineri D, Dianzani C, Cappellano G, Maione F, Baldanzi G, Iacobucci I, Clemente N, *et al.* Osteopontin binds ICOSL promoting tumor metastasis. *Commun Biol* 2020, 3: 615
35. Giopanou I, Kanellakis NI, Giannou AD, Lilis I, Marazioti A, Spella M, Papaleonidopoulos V, *et al.* Osteopontin drives KRAS-mutant lung adenocarcinoma. *Carcinogenesis* 2020, 41: 1134–1144
36. Takano S, Tsuboi K, Tomono Y, Mitsui Y, Nose T. Tissue factor, osteopontin, alphavbeta3 integrin expression in microvasculature of gliomas associated with vascular endothelial growth factor expression. *Br J Cancer* 2000, 82: 1967–1973
37. Szulzewsky F, Schwendinger N, Güneykaya D, Cimino PJ, Hambardzumyan D, Synowitz M, Holland EC, *et al.* Loss of host-derived osteopontin creates a glioblastoma-promoting microenvironment. *Neuro-Oncology* 2018, 20: 355–366
38. Lou H, Wu LQ, Wang H, Wei RL, Cheng JW. The potential role of osteopontin in the pathogenesis of Graves' ophthalmopathy. *Invest Ophthalmol Vis Sci* 2021, 62: 18
39. Liu M, Xu W, Su M, Fan P. REC8 suppresses tumor angiogenesis by inhibition of NF-κB-mediated vascular endothelial growth factor expression in gastric cancer cells. *Biol Res* 2020, 53: 41
40. Guo Z, Huang J, Wang Y, Liu XP, Li W, Yao J, Li S, *et al.* Analysis of expression and its clinical significance of the secreted phosphoprotein 1 in lung adenocarcinoma. *Front Genet* 2020, 11: 547
41. Wang J, Hao F, Fei X, Chen Y. SPP1 functions as an enhancer of cell growth in hepatocellular carcinoma targeted by miR-181c. *Am J Transl Res* 2019, 11: 6924–6937
42. Tang H, Chen J, Han X, Feng Y, Wang F. Upregulation of SPP1 is a marker for poor lung cancer prognosis and contributes to cancer progression and cisplatin resistance. *Front Cell Dev Biol* 2021, 9: 646390
43. Pang X, Zhang J, He X, Gu Y, Qian BZ, Xie R, Yu W, *et al.* SPP1 promotes enzalutamide resistance and epithelial-mesenchymal-transition activation in castration-resistant prostate cancer via PI3K/AKT and ERK1/2 pathways. *Oxid Med Cell Longev* 2021, 2021: 1–15
44. Wei T, Bi G, Bian Y, Ruan S, Yuan G, Xie H, Zhao M, *et al.* The significance of secreted phosphoprotein 1 in multiple human cancers. *Front Mol Biosci* 2020, 7: 565383
45. Deng G, Zeng F, Su J, Zhao S, Hu R, Zhu W, Hu S, *et al.* BET inhibitor suppresses melanoma progression *via* the noncanonical NF-κB/SPP1 pathway. *Theranostics* 2020, 10: 11428–11443
46. Chiu TJ, Lu HI, Chen CH, Huang WT, Wang YM, Lin WC, Li SH. Osteopontin expression is associated with the poor prognosis in patients with locally advanced esophageal squamous cell carcinoma receiving preoperative chemoradiotherapy. *Biomed Res Int* 2018, 2018: 1–9
47. Chen J, Hou C, Zheng Z, Lin H, Lv G, Zhou D. Identification of Secreted phosphoprotein 1 (SPP1) as a prognostic factor in lower-grade gliomas. *World Neurosurg* 2019, 130: e775–e785
48. Blatchley MR, Hall F, Wang S, Pruitt HC, Gerecht S. Hypoxia and matrix viscoelasticity sequentially regulate endothelial progenitor cluster-based vasculogenesis. *Sci Adv* 2019, 5: eaau7518
49. Masoud GN, Li W. HIF-1α pathway: role, regulation and intervention for cancer therapy. *Acta Pharmaceutica Sin B* 2015, 5: 378–389
50. Fu C, An N, Liu J, A. J, Zhang B, Liu M, Zhang Z, *et al.* The transcription factor ZFHX3 is crucial for the angiogenic function of hypoxia-inducible factor 1α in liver cancer cells. *J Biol Chem* 2020, 295: 7060–7074